Calculating the effective delayed neutron fraction in the Molten Salt Fast Reactor: Analytical, deterministic and Monte Carlo approaches

Manuele Aufiero [a], Mariya Brovchenko [b], Antonio Cammi [a], Ivor Clifford [c], Olivier Geoffroy [d], Daniel Heuer [b], Axel Laureau [b], Mario Losa [a], Lelio Luzzi [a,*], Elsa Merle-Lucotte [b], Marco E. Ricotti [a], Hervé Rouch [d]

[a] *Politecnico di Milano, Department of Energy, CeSNEF (Enrico Fermi Center for Nuclear Studies), via Ponzio, 34/3, 20133 Milano, Italy*
[b] *LPSC-IN2P3-CNRS/UJF/Grenoble INP, 53 avenue des Martyrs, 38026 Grenoble Cedex, France*
[c] *Department of Mechanical and Nuclear Engineering, Pennsylvania State University, 324 Reber Building, University Park, PA, USA*
[d] *INOPRO, Téléspace Vercors, 118, chemin des Breux, 38250 Villard de Lans, France*

Received 19 July 2013
Received in revised form 1 October 2013
Accepted 14 October 2013

1. Introduction

The effective delayed neutron fraction (β_{eff}) is an important reactor kinetics parameter. The contribution of delayed neutrons is of primary importance for the safe control of any nuclear reactor. β_{eff} is often adopted as unit of experimental reactivity (*dollar*) (Bell and Glasstone, 1979). Many efforts have been devoted to the measurement (e.g., Sakurai et al., 1999; Rudstam et al., 2002) and calculation (e.g., Meulekamp and van der Marck, 2006; Carta et al., 2011) of physical and effective delayed neutron fractions. The traditional definition of β_{eff} involves the calculation of both the forward and adjoint solution of the neutron transport equations, which makes its accurate calculation by means of continuous energy Monte Carlo codes a hard task, even for static-fuel reactors (Nagaya et al., 2010). In circulating-fuel systems, the motion of delayed neutron precursors complicates the calculation of the effective delayed neutron fraction. In molten salt reactors, the adoption of the Thorium cycle (with ^{233}U as fissile) or the envisaged incineration of Minor Actinides (Merle-Lucotte et al., 2011), and the fuel motion itself (Guerrieri et al., 2013), may lead to β_{eff} values much lower than those typical of Light Water Reactors (LWR). Moreover, loss of flow accidental scenarios in fluid-fuel systems involve the introduction of positive reactivity due to delayed neutron source term redistribution (Guerrieri et al., 2012). The quantification of the introduced reactivity requires the calculation of the difference in delayed neutron effectiveness between static and circulating conditions. For these reasons, accurate and reliable β_{eff} calculations for molten salt reactors are desirable.

In circulating-fuel reactors, the effective delayed neutron fraction (β_{eff}) differs from the physical delayed neutron fraction (β_0) for two distinct reasons. The first reason (common to solid-fuelled reactors) is that the emission spectrum of delayed neutrons is softer than that of prompt neutrons: on average, the former are emitted with a lower energy. This may imply a difference in the importance of delayed and prompt neutrons. The second reason is that delayed neutron precursors are transported by the fluid flow in the fuel circuit and might decay in position of low importance and even out of the core. Spatial effects due to fuel motion are more relevant and always reduce the values of β_{eff}. Energy effects are, in general, of lesser relevance and might reduce or increase the effective delayed neutron fraction, according to the neutronic characteristics of the core.

One-dimensional approaches have often been adopted to correct the effective delayed neutron fraction calculation in order to take into account the fuel motion. One of the most common em-

* Corresponding author. Tel.: +39 0223996326.
E-mail address: lelio.luzzi@polimi.it (L. Luzzi).

Nomenclature

Latin symbols

c	concentration of delayed neutron precursors (m^{-3})
c^*	importance of delayed neutron precursors ($m^{-2}\ s^{-1}$)
cf_{circ}	correction factor for the effective delayed neutron fraction defined in Eq. (1) (–)
D	diffusion coefficient (m)
$D(\mathbf{r}')$	space dependence of the delayed neutron precursors decay probability (–)
D_T	turbulent mass diffusivity ($m^2\ s^{-1}$)
H_a	active height (m)
H_e	extrapolated height (m)
$I(\mathbf{r}')$	space dependence of the neutron importance (–)
$K(\mathbf{r}',\mathbf{r})$	conditional precursor decay probability (–)
k_{eff}	effective multiplication factor (–)
k_p	effective multiplication factor without delayed neutrons (–)
Pr_T	turbulent Prandtl number (–)
r	radial coordinate (m)
R_a	active radius (m)
R_e	extrapolated radius (m)
$S(\mathbf{r})$	space dependence of the precursors source (–)
Sc_T	turbulent schmidt number (–)
T	fuel circulation period (s)
$\mathbf{u}$	fuel velocity field ($m\ s^{-1}$)
z	axial coordinate (m)

Greek symbols

β_0	total physical delayed neutron fraction (–)
β_{eff}	total effective delayed neutron fraction (–)
γ	in-core-to-total fuel volume ratio (–)
λ	decay constant of precursors (s^{-1})
ν	average total number of neutron emitted per fission (–)
ν_T	eddy viscosity ($m^2 s^{-1}$)
Σ_a	absorption cross section (m^{-1})
Σ_f	fission cross section (m^{-1})
Σ_s	scattering cross section (m^{-1})
ϕ	forward neutron flux ($m^{-2}s^{-1}$)
ϕ^*	adjoint neutron flux ($m^{-2}s^{-1}$)
χ_p	delayed neutron yield (–)
χ_p	prompt neutron yield (–)

Superscripts

c	relative to circulating-fuel conditions
s	relative to static-fuel conditions

Subscripts

d	relative to delayed neutrons
g	relative to the gth neutron energy-group
i	relative to the ith delayed neutron precursor group
p	relative to prompt neutrons

Acronyms

CFD	Computational Fluid-Dynamics
EVOL	Evolution and Viability Of Liquid fuel fast reactor systems
IFP	Iterated Fission Probability
LWR	Light Water Reactor
MCNP	Monte Carlo N-Particle transport code
MSFR	Molten Salt Fast Reactor
MSRE	Molten Salt Reactor Experiment
OpenFOAM	Open-source Field Operation And Manipulation
PWR	Pressurized Water Reactor
RANS	Reynolds-Averaged Navier–Stokes
TRU	Transuranic elements

ployed method consists in the correction of static-fuel β_{eff} calculations (obtained by means of commonly available Monte Carlo or deterministic codes, and allowing for energy effects) by means of the fraction of precursors decaying inside the reactor core and not in the out-of-core part of the loop (Lecarpentier, 2001; Cammi et al., 2011; Guerrieri et al., 2013). This fraction is calculated under the hypothesis that the production of precursors has a flat or sinusoidal dependence on the axial coordinate in the core. This approach neglects the effects on β_{eff} due to the inhomogeneous spatial importance of neutrons inside the core. More precisely, this method considers the delayed neutrons produced within the core to have a relative effectiveness of one, regardless of their position, while those produced outside the core have zero importance. On average, precursors are created in a position with a higher spatial neutron importance with respect to the place where they will decay. For this reason, this approach may lead to a significant overestimation of the effective delayed neutron fraction in circulating conditions. In Section 3.1, a new analytical formula for the β_{eff} correction factor is derived, which takes into account the in-core spatial importance effect. Moreover, the proposed approach allows for radial redistribution of the delayed neutron precursors that re-enter in the core.

A more accurate approach involves the adoption of deterministic neutronic calculations to solve the adjoint and forward neutron transport problem. Then, the effective (i.e., adjoint weighted) delayed neutron fraction is calculated. For example, Mattioda et al. (2000) adopted the multi-group neutron diffusion approximation along with precursors drift in one-dimensional geometry. Kópházi et al. (2009) proposed a model for the analysis of moderated MSRs based on neutron diffusion and precursor convection and applied it to the MSRE (Molten Salt Reactor Experiment). In Section 3.2, the solution of the equations of neutron diffusion and precursor transport by means of the multi-physics open-source toolkit OpenFOAM (Weller et al., 1998) is discussed. The proposed solver allows the solution of the forward and adjoint eigenvalue problems for arbitrary geometries based on detailed spatially-dependent velocity fields.

Monte Carlo has often been regarded as reference method for verifying the results of deterministic calculations. Commonly available Monte Carlo codes are not suitable for β_{eff} calculation in circulating-fuel system. Kópházi et al. (2004) evaluated the reactivity loss due to fuel circulation in the MSRE with an extended version of Monte Carlo N-Particle Transport Code (MCNP). In that work, the decay position of delayed neutron precursors was recalculated under simple hypotheses, and neutrons emitted outside of the core were considered lost. More recently, Kiedrowski (2012) also considered the effect of precursors diffusion in fissile solution systems. In both works, the velocity profiles, adopted as input in the Monte Carlo simulations, were simple analytical functions of the position. In Section 3.3, an extension of the Monte Carlo code SERPENT-2 (SERPENT, 2011) for β_{eff} calculation in circulating-fuel systems is presented. The extended version features a suitable algorithm for the transport of delayed neutron precursors. The algorithm is intended for an accurate and efficient tracking of the precursors,

making use of more realistic velocity fields obtained from Computational Fluid Dynamics (CFD) simulations.

The Molten Salt Fast Reactor (MSFR) is adopted as test case for the presented methods. In Section 2, a brief description of the MSFR is given, along with a few details about the different case studies analysed in this work. In Section 3, the three presented methods for β_{eff} calculation are discussed. In Section 4, the main results are reported and discussed. Finally, in Section 5, the main conclusions and possible improvements of the work are presented.

2. Test-case reactor concept

2.1. The Molten Salt Fast Reactor

The Molten Salt Fast Reactor (MSFR) is the reference circulating-fuel reactor in the framework of the Generation IV International Forum (GIF, 2010), and it is mainly developed in the EURATOM EVOL (Evaluation and Viability Of Liquid fuel fast reactor system) Project (EVOL, 2010–2013). Details about the MSFR configuration can be found in the references (Merle-Lucotte et al., 2009, 2011; Brovchenko et al., 2012). In the following, a brief description of the reactor is given. Fig. 1 shows a schematic view of the MSFR components, the fuel salt being not pictured. The molten salt mixture of the fuel circuit acts both as fuel and coolant. The core of the reactor has a volume of 9 m^3. The fuel salt enters from the bottom and is extracted from the top of the core. The heated mixture flows in sixteen external loops where it exchanges heat with an intermediate salt and is pumped back to the core. The fraction of the fuel salt in the core is approximately 50% and the average nominal in-core temperature is 700 °C. Above and below the core, nickel-based alloy reflectors are present in order to improve neutron economy. Radially, the core is surrounded by a fertile salt containing a thorium and lithium fluoride salt, in order to improve the breeding performance of the reactor. In Table 1, the main design parameters of the MSFR are listed. The fuel salt undergoes two types of treatment: an on-line one by neutral gas bubbling in the core and a remote mini-batch reprocessing on-site. The purpose of these salt treatments is to remove most of the fission products without stopping the reactor.

Table 1
Nominal design parameters of the MSFR.

Thermal power	3000 MW
Electrical power	1500 MW
Core inlet temperature	650 °C
Core outlet temperature	750 °C
Fuel salt composition	(^{233}U-started)
$LiF - ThF_4 - {}^{233}UF_4$	77.5–20–2.5 mol%
Fuel salt volume	18 m^3
In-core fuel fraction	50%
Blanket salt composition	(all options)
$LiF - ThF_4$	77.5–22.5 mol%
Fuel salt circulation period	4 s

2.2. Case studies

In Section 4, the effect of both the reactor core shape and the fluid flow path on β_{eff} is discussed. This analysis is carried out by means of a comparison between three different case studies. The first one (referred to as "k-epsilon case study" in the following) concerns the reference MSFR geometry adopted for the neutronic calculation benchmark within the EVOL Project. This option features a simple axial-symmetric (r,z) cylindrical core shape, which can be easily modelled by most of the neutron transport codes (see Fig. 2 and Table 2). The fuel velocity field inside the core is solved adopting the RANS turbulence treatment for incompressible flow and the k-epsilon turbulence model. In nominal conditions, large recirculation vortex appears near the core wall which would lead to excessive structural material temperatures. For this reason, a core shape optimization process is ongoing within the EVOL Project, aimed at the elimination of high-temperature zones. A second configuration (referred to as "uniform velocity case study") is analysed in the present work, as representative of optimized flow path conditions. In this case study, the simplified cylindrical geometry is

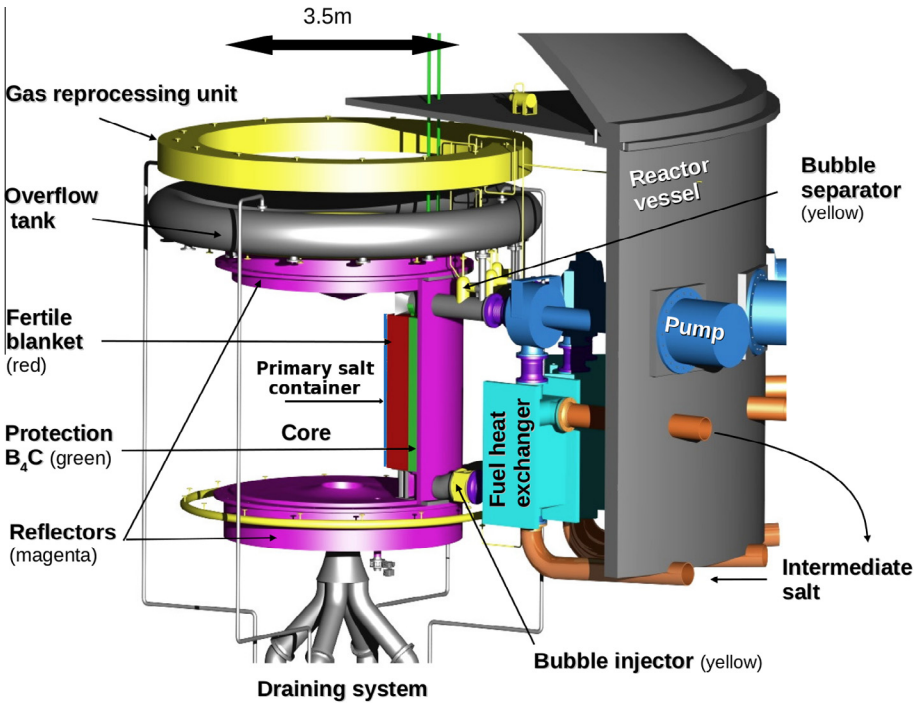

Fig. 1. Schematic representation of the MSFR fuel loop (Brovchenko et al., 2012).

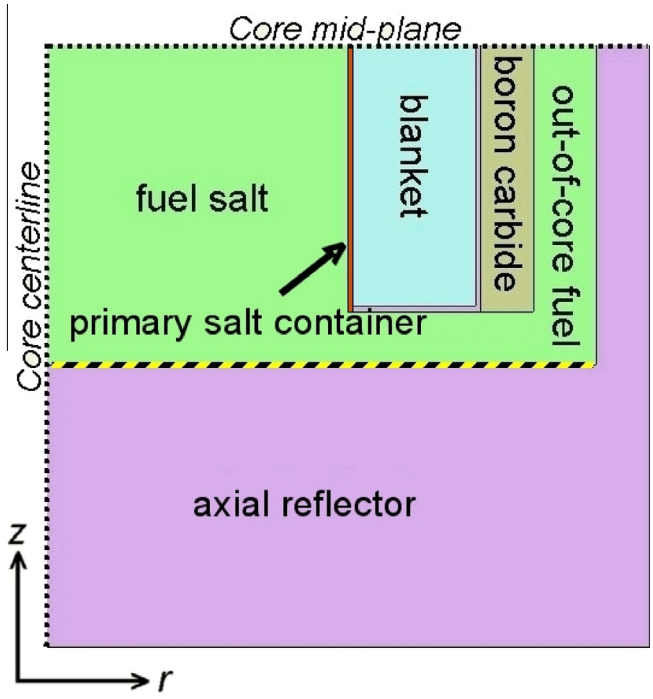

Fig. 2. Simplified axial symmetric (r,z) MSFR geometry.

Table 2
Design parameters of the simplified axial symmetric (r,z) MSFR geometry.

Core diameter	2.25 m
Core height	2.25 m
Blanket thickness	50 cm
Boron carbide layer thickness	20 cm
Axial reflector thickness	1 m

adopted along with a fairly uniform fuel velocity field in the core. Finally, the optimized 3D core shape adopted as CFD benchmark within the EVOL Project is considered as third case study (“optimized geometry, 3D case study”).

Different fuel materials have also been considered for the calculation of the effective delayed neutron fraction in both circulating and static conditions. Thorium is adopted as fertile material in the fuel mixture. As fissile material the following options have been studied: (i) ^{235}U at 20% at. enrichment; (ii) only ^{233}U; (iii) a mixture of transuranic (TRU) elements from PWR spent fuel; and (iv) a mixture of transuranic elements and ^{235}U at 13% at. enrichment. Details about the (iii) and (iv) fuel isotopic compositions can be found in (Merle-Lucotte et al., 2009, 2013).

3. Methods

In this section, the three proposed approaches adopted to calculate the effective delayed neutron fraction in the MSFR are described.

3.1. Analytical approach

In the following, an analytical formula for the circulating-to-static correction factor of the effective delayed neutron fraction is derived. It features an explicit consideration of the in-core spatial neutron importance. This leads to significant difference with respect to non-adjoint-weighted approaches (see Fig. 6).

We can write the correction factor for the effective delayed neutron fraction as:

$$cf_{circ} \equiv \frac{\beta_{eff}^{c}}{\beta_{eff}^{s}} = \frac{\int_{core} D^{c}(\mathbf{r}') \cdot I^{c}(\mathbf{r}')\, d\mathbf{V}'}{\int_{core} D^{s}(\mathbf{r}') \cdot I^{s}(\mathbf{r}')\, d\mathbf{V}'} \tag{1}$$

where $D^{c}(\mathbf{r}')$ and $D^{s}(\mathbf{r}')$ are the probabilities to have a precursors decay in the position $\mathbf{r}'$ in circulating and static conditions, respectively, and $I(\mathbf{r}')$ is the spatial dependence of the neutron importance.

We can write $D(\mathbf{r}')$ as:

$$D(\mathbf{r}') = \int_{core} K(\mathbf{r}', \mathbf{r})\, S(\mathbf{r})\, d\mathbf{V} \tag{2}$$

where $S(\mathbf{r})$ is the probability to have the production of a precursor in the position $\mathbf{r}$ and $K(\mathbf{r}', \mathbf{r})$ is the kernel function of the integral transform operator that allows transforming the probability density function of the precursor production into the probability density function of the precursor decay. In a simpler way, $K(\mathbf{r}', \mathbf{r})$ can be seen as the conditional probability to have the decay of a precursor in the position $\mathbf{r}'$, given that it was produced in the position $\mathbf{r}$. $K(\mathbf{r}', \mathbf{r})$ is independent from $S(\mathbf{r})$ and $I(\mathbf{r}')$ and depends only on the precursor decay constant and the fluid-fuel flow.

For the static-fuel conditions, any delayed neutron precursors will decay where it has been created:

$$K^{s}(\mathbf{r}', \mathbf{r}) = \delta(\mathbf{r}' - \mathbf{r}) \tag{3}$$

thus

$$D^{s}(\mathbf{r}') = S^{s}(\mathbf{r}') \tag{4}$$

Now, we can rewrite Eq. (1) as:

$$cf_{circ} = \frac{\int_{core} \int_{core} [K^{c}(\mathbf{r}', \mathbf{r})\, S^{c}(\mathbf{r})\, d\mathbf{V}] I^{c}(\mathbf{r}')\, d\mathbf{V}'}{\int_{core} S^{s}(\mathbf{r}') \cdot I^{s}(\mathbf{r}')\, d\mathbf{V}'} \tag{5}$$

Due to the fact that delayed neutrons are very few compared to prompt neutrons, we can consider that the spatial source of precursors (that are mainly produced by prompt neutrons) is the same for static and circulating cases. We have that: $S^{c}(\mathbf{r}) \simeq S^{s}(\mathbf{r}) \simeq S(\mathbf{r})$.

Under the one-group neutron diffusion hypotheses, recalling again that delayed neutrons are few compared to prompt neutrons, we have that the spatial dependence of the neutron flux and the adjoint flux is the same: $\phi(\mathbf{r}') \simeq \phi^{*}(\mathbf{r}')$. In the case of homogeneous core composition the source of delayed neutrons is proportional to the neutron flux and the spatial neutron importance is proportional to the adjoint flux.

Under these hypotheses, in the case of a cylindrical core, we obtain:

$$S(\mathbf{r}) \simeq I(\mathbf{r}) \simeq \cos\left(\frac{\pi z}{H_e}\right) J_0\left(\frac{2.405\, r}{R_e}\right) \tag{6}$$

where H_e and R_e are the extrapolated height and radius, respectively, at which ϕ and ϕ^{*} go to zero. $S(\mathbf{r})$ and $I(\mathbf{r})$ are both normalized to be equal to one at core centre.

Now, only the term $K^{c}(\mathbf{r}', \mathbf{r})$ is missing in Eq. (5). In the following, $K^{\lambda T}(r'z' \leftarrow rz)$ is derived for the general case of precursor decay constant λ, fuel salt loop circulation period T and in-core-to-total fuel volume ratio γ. H_a and R_a are the core active height and radius, respectively. As further hypotheses, uniform (axial) velocity in the core and complete mixing in the out-of-core part of the primary loop (i.e., in the pump and the heat exchanger) have been assumed.

In order to simplify the solution, we can split the problem in two parts:

$$K^{\lambda T}(r'z' \leftarrow rz) = p_1^{\lambda T}(r'z' \leftarrow rz) + p_2^{\lambda T}(r'z' \leftarrow rz) \tag{7}$$

where $p_1^{\lambda T}(r'z' \leftarrow rz)$ is the conditional probability for the decay in $(r'z')$ during the first passage in the core and $p_2^{\lambda T}(r'z' \leftarrow rz)$ is the

probability to have a decay during the further N passage in the core, with $N \to \infty$.

In general, for a precursor created at time $t = 0$, the probability to have a decay between t_1 and $t_1 + \varepsilon$ is: $p = \int_{t_1}^{t_1+\varepsilon} \lambda e^{-\lambda t}\, dt$ for $t_1 \geqslant 0$ and $p = 0$ for $t_1 < 0$. Similarly, the probability density function for a precursor created in z to have a decay, during the first loop, in z' is:

$$p(z' \leftarrow z) = \int_{T\gamma\frac{z'-z}{H_a}}^{T\gamma\left(\frac{z'-z}{H_a}+\frac{dz'}{H_a}\right)} \lambda e^{-\lambda t}\, dt \tag{8}$$

for $z' \geqslant z$ and $p = 0$ for $z' < z$. Thus, due to the zero radial velocity in the core, we have:

$$\begin{aligned} p_1^{\lambda T}(r'z' \leftarrow rz) &= \frac{1}{2\pi r}\delta(r'-r)dr' \cdot \int_{T\gamma\frac{z'-z}{H_a}}^{T\gamma\left(\frac{z'-z}{H_a}+\frac{dz'}{H_a}\right)} \lambda e^{-\lambda t}\, dt \\ &= \frac{1}{2\pi r}\delta(r'-r)dr' \cdot e^{-\lambda T\gamma\frac{z'-z}{H_a}}\left(1 - e^{-\lambda T\gamma\frac{dz'}{H_a}}\right) \end{aligned} \tag{9}$$

It can be shown that the limit of $p_1^{\lambda T}$ for $\lambda T \to +\infty$ is:

$$\lim_{\lambda T \to +\infty} p_1^{\lambda T}(r'z' \leftarrow rz) = \frac{1}{2\pi r}\delta(r'-r)dr' \cdot \delta(z'-z)dz' \tag{10}$$

Then, as expected, for very low fuel velocity the decay will occur near the precursor production position. The limit for very fast fuel velocity ($\lambda T \to 0^+$) is:

$$\lim_{\lambda T \to 0^+} p_1^{\lambda T}(r'z' \leftarrow rz) = 0 \tag{11}$$

It means that the probability to have a decay during the first passage in the core tends to zero as fuel velocity increases.

For finite value of λT, we can proceed to first order Taylor series expansion around $dz' = 0$:

$$p_1^{\lambda T}(r'z' \leftarrow rz) = \frac{1}{2\pi r}\delta(r'-r)dr' \cdot e^{-\lambda T\gamma\frac{z'-z}{H_a}} \cdot \lambda T\gamma\frac{dz'}{H_a} \tag{12}$$

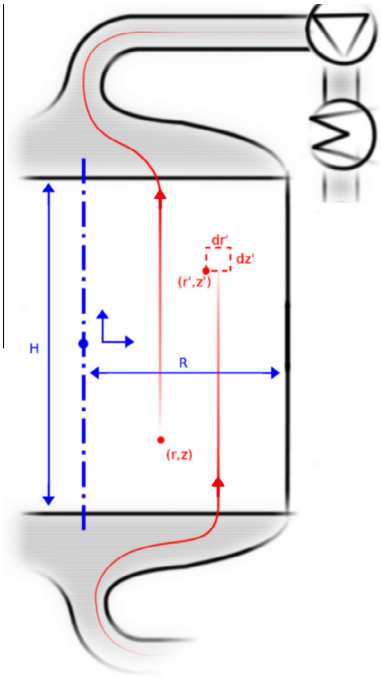

Fig. 3. Schematic representation of the reactor model adopted in the derivation of the analytical approach.

After the first loop, if the precursor has not yet undergone the decay, it might emit the neutron in the out-of-core part of the fuel loop or come back in the core at $z' = -\frac{H_a}{2}$ in any radial position (see Fig. 3). If the precursor is still alive after the second passage in the core, it might decay outside or come back again at $z' = -\frac{H_a}{2}$, and so on:

$$\begin{aligned} p_2^{\lambda T}(r'z' \leftarrow rz) = \frac{2\pi r'dr'}{\pi R_a^2} \cdot \Bigg[&\int_{T\gamma\frac{z'-z}{H_a}+T}^{T\gamma\left(\frac{z'-z}{H_a}+\frac{dz'}{H_a}\right)+T} \lambda e^{-\lambda t}\, dt + \int_{T\gamma\frac{z'-z}{H_a}+2T}^{T\gamma(\ldots)+2T} \lambda e^{-\lambda t}\, dt \\ &+ \int_{T\gamma\frac{z'-z}{H_a}+3T}^{T\gamma(\ldots)+3T} \lambda e^{-\lambda t}\, dt + \ldots \Bigg] \end{aligned} \tag{13}$$

$p_2^{\lambda T}(r'z' \leftarrow rz)$ can be rewritten as:

$$p_2^{\lambda T}(r'z' \leftarrow rz) = \frac{2\pi r'dr'}{\pi R_a^2} \cdot \left(\sum_{N=1}^{\infty} e^{-N\lambda T} \right) e^{-\lambda T\gamma\frac{z'-z}{H_a}}\left(1 - e^{-\lambda T\gamma\frac{dz'}{H_a}}\right) \tag{14}$$

The limit for very low fuel velocity ($\lambda T \to +\infty$) is:

$$\lim_{\lambda T \to +\infty} p_2^{\lambda T}(r'z' \leftarrow rz) = 0 \tag{15}$$

As λT tends to $+\infty$, the probability to have a decay during a passage in the core different from the first one tends to zero.

The sum $\sum_{N=1}^{\infty} e^{-N\lambda T}$ converges to $\frac{1}{e^{\lambda T}-1}$ and we obtain:

$$p_2^{\lambda T}(r'z' \quad rz) = \frac{2\pi r'dr'}{\pi R_a^2} \cdot \frac{1}{e^{\lambda T} - 1} \cdot e^{-\lambda T\gamma\frac{z'-z}{H_a}}\left(1 - e^{-\lambda T\gamma\frac{dz'}{H_a}}\right) \tag{16}$$

The limit of $p_2^{\lambda T}$ for $\lambda T \to 0^+$ is:

$$\lim_{\lambda T \to 0^+} p_2^{\lambda T}(r'z' \leftarrow rz) = \gamma \cdot \frac{2\pi r'dr'}{\pi R_a^2} \cdot \frac{dz'}{H_a} \tag{17}$$

For very fast fuel velocity, the probability to have a precursor decay in a certain position becomes uniform in the core and all the dependencies on the production position are lost. As expected, as λT tends to 0^+, the integral probability to have a decay inside the core tends to the in-core-to-total volume ratio γ.

After first order expansion of $p_2^{\lambda T}$ around $dz' = 0$, we can finally write the general expression for $K^{\lambda T}$:

$$\begin{aligned} K^{\lambda T}(r'z' \leftarrow rz) = p_1^{\lambda T}(r'z' \leftarrow rz) + p_2^{\lambda T}(r'z' \leftarrow rz) = e^{-\lambda T\gamma\frac{z'-z}{H_a}} \\ \cdot \lambda T\gamma\frac{dz'}{H_a}\left[H(z'-z) \cdot \frac{1}{2\pi r}\delta(r'-r)dr' + \frac{1}{e^{\lambda T}-1} \cdot \frac{2\pi r'dr'}{\pi R_a^2}\right] \end{aligned} \tag{18}$$

where $H(z'-z)$ is the heavyside step function defined as $\int_{-\infty}^{z'} \delta(s-z)\, ds$ and is zero for $(z' < z)$ and one for $(z' > z)$.

Now, all the terms of Eq. (5) are known and the correction factor can thus be calculated for any λT. The values of the parameters for the MSFR are: $H_a = 2.24$ m, $R_a = 1.12$ m, $H_e = 2.6$ m, $R_e = 1.3$ m, $\gamma = 0.5$.

3.2. Deterministic approach

The second approach adopted in the present work involves the solution of the forward and adjoint multi-group diffusion eigenvalue problems, along with precursor transport using CFD techniques. In this context, the fluid velocity field enters as an external operator in the system of equations (Mattioda et al., 2000; Lapenta et al., 2001) for the convective transport of the delayed neutron precursors. Commonly available neutronics codes (used for solid-fuelled systems) are unable to model this convective transport and are therefore not suitable. For this reason, the multi-physics open-source toolkit OpenFOAM (Weller et al., 1998) is adopted to spatially discretize and numerically solve the equations related to multi-group neutron diffusion and neutron precursor transport using standard finite-volume methods. The coupled solution of the multi-group neutron diffusion equation within this framework is based on the work of Clifford and Jasak

(2009). The fluid flow inside the reactor core has been obtained adopting the SIMPLE algorithm for incompressible flows along with RANS turbulence treatment. In particular, the standard k-epsilon turbulence model available in OpenFOAM has been adopted. In the present work, the spatially-dependent fluid velocity field is considered to be a fixed input to the neutronics calculation. Calculations refer to "zero-power" conditions and temperature feedbacks to both the fluid flow and the neutronics have been neglected. In the following, the equations implemented in the developed solver are reported.

$$\nabla\cdot D_g\nabla\phi_g-\Sigma_{a,g}\phi_g-\sum_{g'\neq g}\Sigma_{s,gg'}\phi_g+\sum_{g'\neq g}\Sigma_{s,g'g}\phi_{g'}+(1-\beta_0)\chi_{p,g}\sum_{g'=1}^{6}\frac{1}{k_{eff}}(\nu\Sigma_f)_{g'}\phi_{g'}+\sum_{i=1}^{8}\chi_{d,g}\lambda_i c_i=0 \tag{19}$$

$$-\nabla(\mathbf{u}c_i)+\nabla\cdot\frac{\nu_T}{Sc_T}\nabla c_i-\lambda_i c_i+\beta_{0,i}\sum_{g=1}^{6}\frac{1}{k_{eff}}(\nu\Sigma_f)_g\phi_g=0 \tag{20}$$

Eqs. (19) and (20) are related to the forward eigenvalue problem. Here, the delayed neutron source ($\sum_{i=1}^{8}\chi_{d,g}\lambda_i c_i$) is explicitly written as function of the precursors concentration (c_i) and decay constants (λ_i), which is not usually the case in solid fuel eigenvalue problems, where the delayed neutron source term can be eliminated in the neutron balance. In fact, the eigenvalue solution is independent of the decay constants of the delayed neutron precursors only in static-fuel cases. The first two terms of the delayed neutron precursor balance equations (Eq. 20) represent the convection and diffusion of fission products responsible for neutron emissions. $\mathbf{u}$ is the fuel velocity field and ν_T is the turbulent viscosity. These fields are calculated in OpenFOAM, before starting the power iteration solution of the eigenvalue problem. The turbulent Schmidt number (Sc_T) is defined as the ratio of the turbulent momentum diffusivity (eddy viscosity) ν_T and the turbulent mass diffusivity D_T:

$$Sc_T=\frac{\nu_T}{D_T} \tag{21}$$

Sc_T can be seen as the equivalent of the turbulent Prandtl number (Pr_T) for mass transport and is commonly adopted in CFD calculations to model the species diffusion (Tominaga and Stathopoulos, 2007). Due to the unavailability of accurate studies on turbulent mass transport in the MSFR carrier salt and operating conditions, a tentative value of 1 has been adopted for Sc_T. A sensitivity analysis to the value of Sc_T for one case study is presented in Section 4.

The laminar diffusion coefficients of the different chemical species constituting delayed neutron precursors have not been measured for the MSFR carrier salt. In general, diffusion coefficients in molten fluorides at operating temperature typical of nominal reactor conditions are very low (Salanne et al., 2009; Rollet et al., 2010) compared to turbulent diffusivity. For this reason, the laminar diffusion of the precursors has been neglected in the present work. Moreover, some of the delayed neutron precursors are constituted by metallic species that are not soluble in the molten fluoride matrix. These precursors may leave the fuel circuit due to extraction by gas bubbling or deposition in cold metallic surfaces in the out-of-core part of the loop. According to previous studies (Doligez, 2010), the extraction will affect at most about 1% of the precursors before delayed neutron emission, in the nominal MSFR conditions.

Hereafter, the equations related to the adjoint eigenvalue problem are presented:

$$\nabla\cdot D_g\nabla\phi_g^*-\Sigma_{a,g}\phi_g^*+\sum_{g'\neq g}\Sigma_{s,gg'}\phi_g^*-\sum_{g'\neq g}\Sigma_{s,g'g}\phi_{g'}^*+(1-\beta_0)\frac{1}{k_{eff}}(\nu\Sigma_f)_g\cdot\sum_{g'=1}^{6}\chi_{p,g'}\phi_{g'}^*+\frac{1}{k_{eff}}(\nu\Sigma_f)_g\cdot\sum_{i=1}^{8}\beta_{0,i}c_i^*=0 \tag{22}$$

$$-\nabla(-\mathbf{u}c_i^*)+\nabla\cdot\frac{\nu_T}{Sc_T}\nabla c_i^*-\lambda_i c_i^*+\lambda_i\sum_{g=1}^{6}\chi_{d,g}\phi_g^*=0 \tag{23}$$

c_i^* (Eqs. (22) and (23)) is not present in classical solid fuel adjoint problem. It represents the importance of a precursor injected in a certain position (i.e., it is the average importance of the delayed neutrons emitted).

In the present work, the six energy-groups structure employed in previous works (Fiorina et al., 2013) has been adopted and it is reported in Table 3. The JEFF-3.1 evaluated nuclear data library (Koning et al., 2006) has been adopted for the delayed neutron group decay constants and physical fractions. This library adopts eight groups of precursors, with the same time constants for any fissioning isotope. In Table 4, the decay constants of the different groups are reported along with the physical fractions ($\beta_{0,i}/\beta_{0,tot}$) for some fissile isotopes. The value of the cross sections, diffusion coefficients and neutron emission spectra have been calculated by means of the SERPENT Monte Carlo code (SERPENT, 2011), adopting the same library.

The Open-source Field Operation And Manipulation (OpenFOAM) framework is a C++ library providing automatic matrix construction and solution for scalar and vector equations using standard finite-volume approaches based on user-specified differencing and interpolation schemes. The flexibility of design makes this library ideal for modelling complex coupled problems. The framework has been applied extensively for CFD simulations. An attractive feature of the OpenFOAM framework is that the top-level C++ representations of continuum mechanics equations closely parallel their mathematical descriptions. Clifford and Ivanov (2010) extended OpenFOAM to provide a top-level presentation for the implicit solution of multiple coupled variables, based on the block-coupled solver implementation of Clifford and Jasak (2009), which is particularly suited to the solution of the multi-group neutron diffusion equation. Eq. (19), in vector form, is discretized and solved for all six energy-groups using the following line of source code:

```
solve
(
  - blockFvm::laplacian (D, phi)
   + blockFvm::Sp (sigma_a - sigma_s, phi)
  ==
      (1-beta_tot)/k_eff*((chi_p*(nu_tot &
  sigma_f)) & phi)
  + (chi_d*delayedNeutronSource)
);
```

Neumann conditions are applied to the forward and adjoint precursor equations at the boundaries of the fuel salt domain. The albedo boundary condition has been applied to the neutron diffusion Eqs. (19) and (22), with the albedo coefficients calculated from Serpent results.

The bi-conjugate gradient solution algorithm with ILU preconditioning has been used for all equations. The traditional power iteration method has been employed for the steady-state nonlinear eigenvalue solution for both the forward and adjoint cases. Here the fission rate and delayed neutron precursor concentrations from the previous iteration are supplied as source terms for the solution

Table 3
6 energy-groups structure adopted in the deterministic approach.

Energy-group #	1	2	3	4	5	6
Upper energy boundary (MeV)	7.485×10^{-4}	5.531×10^{-3}	2.479×10^{-2}	4.979×10^{-1}	2.231	20

Table 4
Decay constants of delayed neutron precursors. Physical delayed neutron fractions of some isotopes are also reported, for incident neutron energy of 1 eV. JEFF-3.1 nuclear data library.

Delayed neutron group #	1	2	3	4	5	6	7	8
Decay constant (s^{-1})	1.25×10^{-2}	2.83×10^{-3}	4.25×10^{-2}	1.33×10^{-1}	2.92×10^{-1}	6.66×10^{-1}	1.63	3.55
	Relative physical fractions (%) ($\beta_{0,i}/\beta_{0,tot}$)							
U-235	3.4	15.0	9.9	20.0	31.2	9.3	8.8	2.4
U-233	8.0	15.7	13.4	20.9	30.8	3.7	6.2	1.3
Pu-239	2.9	22.5	9.5	14.9	35.1	3.7	9.7	1.7

of the multi-group neutron diffusion equation.

Once the forward and adjoint problems have been solved, the effective delayed neutron fractions can be calculated as follows (Mattioda et al., 2000):

$$\beta_{eff,i} = \frac{\int \sum_{g=1}^{6} \phi_g^* \chi_{d,g} \lambda_i c_i}{\int \sum_{g=1}^{6} \phi_g^* \chi_{d,g} \sum_{k=1}^{8} \lambda_k c_k + \int \sum_{g=1}^{6} \phi_g^* \chi_{p,g} \sum_{g'=1}^{6} \phi_{g'} (\nu \Sigma_f)_{g'}} \quad (24)$$

In Fig. 4, the velocity field and stream lines of three different cases (see Section 2.2) are presented. On the top left, the axial-symmetric solution of the velocity field obtained with k-epsilon turbulence model is shown for the nominal flow rate conditions in the axial-symmetric MSFR geometry. On the top right, the case study with uniform in-core velocity is shown as representative of conditions of optimized fluid flow path. On the bottom, results obtained in the full-core optimized geometry with the k-epsilon turbulence model are shown. The effects of recirculation vortex and core geometry are discussed in Section 4.

3.3. Monte Carlo approach

The third approach presented is based on the continuous energy Monte Carlo method. The Monte Carlo code SERPENT-2 (SERPENT, 2011) has been extended, in order to take into account the presence of a circulating fuel. In common Monte Carlo criticality source simulations, when the emission of a delayed neutron is sampled, this affects only the energy of the new particle, which is sampled according to the emission spectrum of the particular delayed neutron group. In the extended version, the initial position of the new history is corrected according to the fuel velocity field and the de-

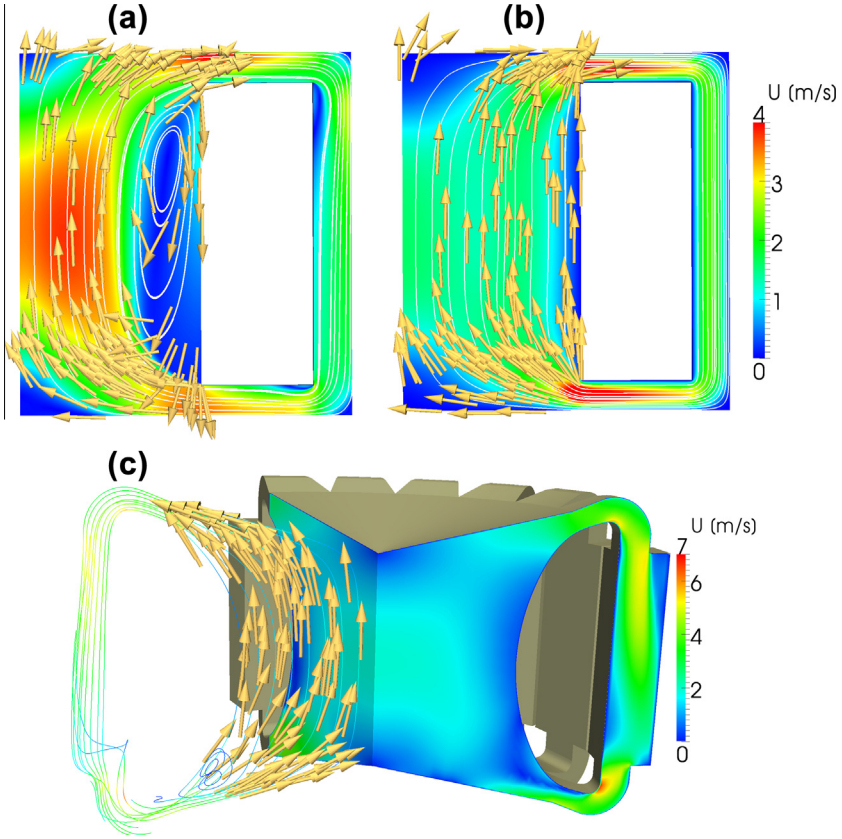

Fig. 4. Stream lines and velocity fields of the 3 analysed cases: (a) k-epsilon case study, (b) uniform velocity case study, and (c) optimized geometry, 3D case study.

layed neutron emission time, which is sampled according to the group decay constant.

As tracking algorithm, a fifth-order Runge–Kutta explicit integrator with embedded fourth-order error estimation is adopted (Dormand and Prince, 1980). The velocity fields employed have been calculated by means of OpenFOAM, adopting the k-epsilon turbulence model, and mapped to an axial-symmetric cartesian mesh. The adoption of an error estimation technique allows a continuous correction of the tracking time-step, according to the adopted mesh and the input velocity field. In principle, an *a priori* choice of the time-step is a difficult task. Independent of the particular integration algorithm adopted, if too long time-steps are employed, tracking errors might lead to inaccurate results due to a wrong spatial distribution of the delayed neutron source. On the other hand, the adoption of too short time-steps might lead to an unacceptable increase of the computational time. Nonetheless, the choice of the tolerance adopted for error check and adaptive time-stepping, is still a delicate task.

In the following, the algorithm adopted in SERPENT-2 for the transport of delayed neutron precursors is reported:

When the emission of a delayed neutron is sampled:
(1) Sample the delayed neutron group according to the physical delayed neutron fractions $\beta_{0,i}$
(2) Sample the neutron emission time EM_{time} according to the decay constant λ_i
(3) Start the precursors tracking loop
$TRK_{time} = 0$
$\Delta t = \Delta t_{zero}$ (initial guess)
(4) while ($TRK_{time} < EM_{time}$)
(5) for all the **k** stages of the Dormand-Prince algorithm
(6) Calculate $\mathbf{u}_k^x$, $\mathbf{u}_k^y$, $\mathbf{u}_k^z$ from the Cartesian mesh
(7) Calculate the new precursor position at the end of the time-step Δt
(8) Calculate the tracking error estimation ERR
(9) if ($ERR < \varepsilon_{min}$) where ε_{min} is a user defined tolerance
(10) Increase the time-step Δt
(11) if ($ERR > \varepsilon_{max}$) where ε_{max} is a user defined tolerance
(12) Reduce the time-step Δt
(13) $TRK_{time} = TRK_{time} + \Delta t$
(14) Sample the new neutron energy according to the delayed neutron group
Start the new neutron history

Unfortunately, the availability of the correct energy and spatial distribution of the delayed neutrons is not enough to guarantee an accurate estimation of the delayed neutron fraction. As already mentioned, β_{eff} is an adjoint-weighted quantity and cannot be estimated by means of a simple criticality source simulation. A detailed review of the different techniques for effective delayed neutron fraction calculation in Monte Carlo is out of the scope of the present work. In the following, two of the most commonly adopted methods and their applicability are briefly discussed. More complete and detailed analyses of different methods can be found in Meulekamp and van der Marck (2006), Nagaya et al. (2010).

Often, β_{eff} is estimated through the prompt method. This method involves two separated Monte Carlo simulations, with and without the production of delayed neutrons. The effective delayed neutron fraction is then approximated as:

$$\beta_{eff} \simeq 1 - \frac{k_p}{k_{eff}} \tag{25}$$

where k_{eff} is the effective multiplication factor of the reference case and k_p is the effective multiplication factor of the simulation without delayed neutrons.

This method can be easily adopted without any modification of the available Monte Carlo codes but requires a relatively high amount of computational resources. Due to the fact that the effective delayed neutron fraction is obtained by comparison of two separate runs, to have a relative statistical error on β_{eff} in the order of 1%, k_{eff} estimations with an accuracy of few *pcm* are required. Moreover, if the effective contributions of the different delayed neutron groups need to be investigated, the prompt method looses any applicability due to the presence of $\beta_{eff,i}$ fractions as low as few *pcm*, whose contributions would be highly covered by uncertainty in k_{eff} estimations.

Other approaches, which employ a single simulation and involve the approximation of the adjoint weighting function, have been developed. The Meulekamp and van der Marck (2006) method approximates the neutron importance to the probability of producing a fission (next fission probability). It captures very well the difference in importance between prompt and delayed neutrons due to energy spectra but is not suitable when relevant spatial effects are present (Nagaya et al., 2010) and gives wrong results in circulating-fuel conditions.

For this reason, the Iterated Fission Probability (IFP) method (Nauchi and Kameyama, 2010; Kiedrowski et al., 2011) has been implemented in SERPENT-2. This method allows to calculate directly adjoint-weighted quantities. In Fig. 5, the comparison between the different β_{eff} estimations is shown. Results are relative to the MSFR nominal conditions (k-epsilon case study). The IFP method converges to the "prompt" method in about 20 latent generations. The Meulekamp and van der Marck (2006) method fails to give a good approximation of β_{eff}. The details of the IFP method implementation in SERPENT-2 can be found in Leppänen et al. (2013).

In order to better compare the analytical results with Monte Carlo simulations in the limit of infinite fuel velocity ($\lambda T \to 0$), a further modification of the code has been implemented. As already discussed, in case of infinite fuel velocity, any precursors that is produced has a uniform decay probability in the whole fuel loop. In this case, the starting positions of the delayed neutrons are uniformly sampled in the entire reactor geometry. If the sampled point is in the fuel circuit, the position is accepted and the new neutron history is started. If the sampled point falls in a different material (e.g., reflector, neutron shield, etc.), the position is rejected and new random coordinates are extracted.

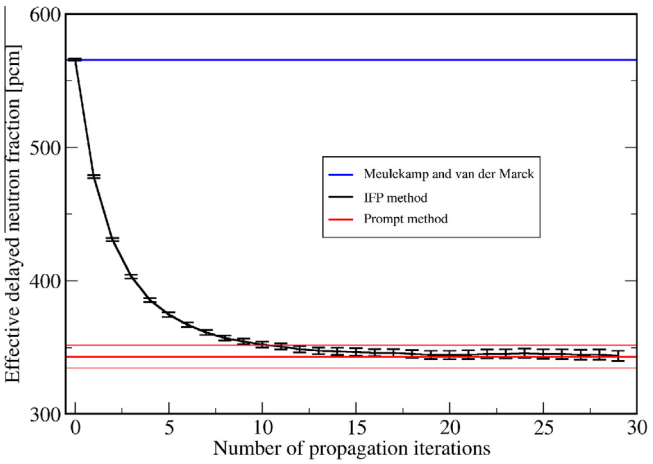

Fig. 5. Comparison between IFP, "prompt" and Meulekamp methods (U235-started, k-epsilon case study; nominal flow rate).

The MSFR features the presence of radial blankets constituted by a mixture of Thorium-fluoride and Lithium-fluoride. Recent studies highlighted the necessity to actively remove the energy released in the blanket material by flowing the fluid in an external circuit. At present, no detailed studies are available on this subject. However, only few fissions occur in the blanket and few delayed neutrons are produced there. Moreover, these neutrons feature a very low importance because are likely to undergo radiative capture in the fertile material. For these reasons, precursor motion is neglected in the blanket material, and any delayed neutron produced there is emitted in the position of the originating fission event.

4. Numerical results and discussion

In this section, the presented approaches are adopted to calculate the effective delayed neutron fraction in the Molten Salt Fast Reactor.

In Fig. 6, the correction factor calculated by means of the three proposed approaches is presented, as function of the dimensionless parameter λT (see Section 3.1). Results are relative to the uniform velocity case study (see Fig. 4). Results show good agreement over a wide range of λT values. It is clear that, in this case, even a simple analytical approach is able to accurately estimate the effective delayed neutron fraction, provided that a correct spatial adjoint-weighting function is adopted. For comparison, results from one of the commonly adopted 1-D approach (non-adjoint-weighted) are presented (Lecarpentier, 2001). This and other similar methods overestimate the correction factor over the whole range of λT values, with relative errors up to 20–30%. For small values of λT, precursors are tracked for several loops over the fuel circuit in the Monte Carlo approach. In this case, tracking errors accumulate and a small bias in the estimation may arise. Nonetheless, the limit for $\lambda T \to 0$ can be studied with a simplified algorithm (see Section 3.3). The yellow dot shows the IFP estimation of the β_{eff} correction factor obtained with uniform sampling of the delayed neutron position in the fuel. In this case, the three methods are again in good agreement. In the top of the plot, the positions of delayed neutron constants of the JEFF-3.1 library are shown for a circulating period of 4 s (nominal MSFR flow rate).

In Fig. 7, results from the k-epsilon case study with axial-symmetric geometry are presented. In this case, the analytical estimations significantly differ from those of OpenFOAM and SERPENT. This is due to the inability of the simplified approach to capture the effects of in-core fuel recirculation (see Fig. 4), both at high and low values of λT.

These results help in the interpretation of the effect of recirculation vortex on β_{eff}. At low λT (high recirculation velocity), the main effect is the higher in-core retention of precursors (see Fig. 8). Precursors are trapped in the core and this leads to higher values of the effective delayed neutron fractions for slow-decaying groups, even if the recirculation zone presents a relatively low importance. For high values of λT, most of the precursors would decay inside the core independently of the presence of the vortex. In this case, the main effect of the vortex is the increase of the effective fuel velocity at core centre (for a given flow rate). This leads to a faster removal of precursors from central zones of high neutron importance and the effect is a reduced $\beta_{eff,i}$ for fast-decaying groups.

In Fig. 8, the concentration (top) and importance (bottom) of delayed neutron precursors are shown for different values of the dimensionless parameter λT. In the recirculation zone, the increase in both concentration and importance of delayed neutron precursors is evident for low values of λT.

In Fig. 9, the effect of turbulent diffusion is analysed. The turbulent Schmidt number Sc_T is the ratio between the eddy viscosity and the eddy diffusivity and is adopted to take into account the effects of turbulent mixing (i.e., equivalent of Pr_T for mass transport). Uncertainties are present both in the evaluation of the turbulent viscosity field by means of RANS turbulence models and in the choice of an appropriate value for Sc_T. For this reason, a sensitivity to the effect of turbulent diffusion is presented for the nominal flow rate conditions. The main effect of turbulent diffusion is to reduce the retention of delayed neutron precursors in the recirculation zone. This leads to a decrease of the effective delayed neutron fraction for low Sc_T values, as delayed neutron are more likely to be emitted in the out-of-core part of the fuel loop. The effect of the turbulent diffusion term becomes very small in case of no recirculation vortex. Nonetheless, the analysed case studies highlight the important role of fluid flow modelling inside the reactor core. A proper solution of the in-core flow path (e.g., by means of CFD simulations) appears to be a first mandatory step, while calculating the effective delayed neutron fraction in circulating fuel reactors.

The adoption of the dimensionless parameter λT allows a better comprehension of the phenomena governing the reduction of the effective delayed neutron fraction and ensures a more accurate

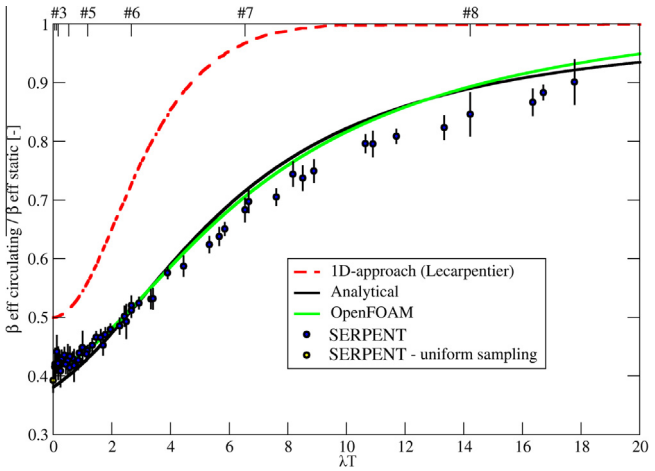

Fig. 6. Correction factor: comparison between analytical approach, SERPENT and OpenFOAM (uniform velocity case study).

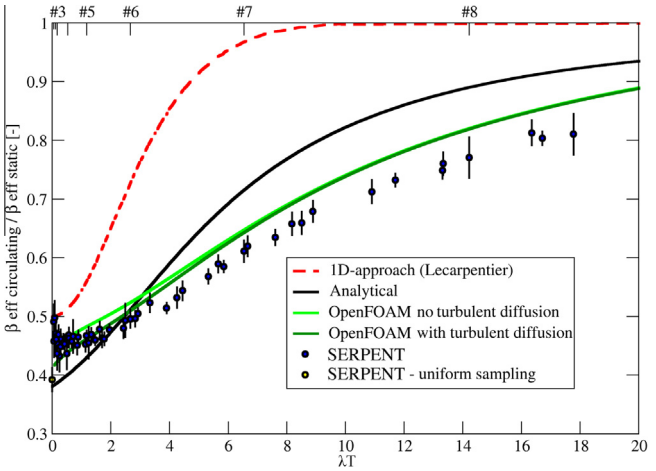

Fig. 7. Correction factor: comparison between analytical approach, SERPENT and OpenFOAM (k-epsilon case study).

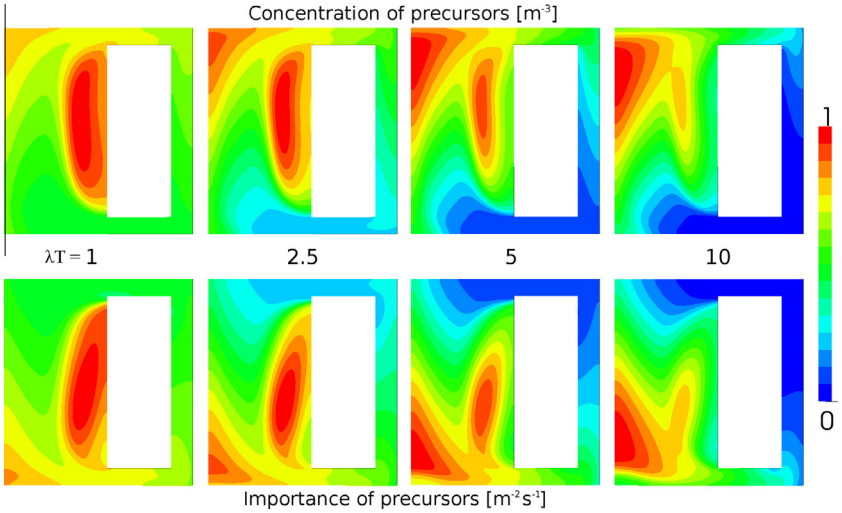

Fig. 8. Precursor concentration and importance for the k-epsilon case study for different values of the dimensionless parameter λT (OpenFOAM; arbitrary units).

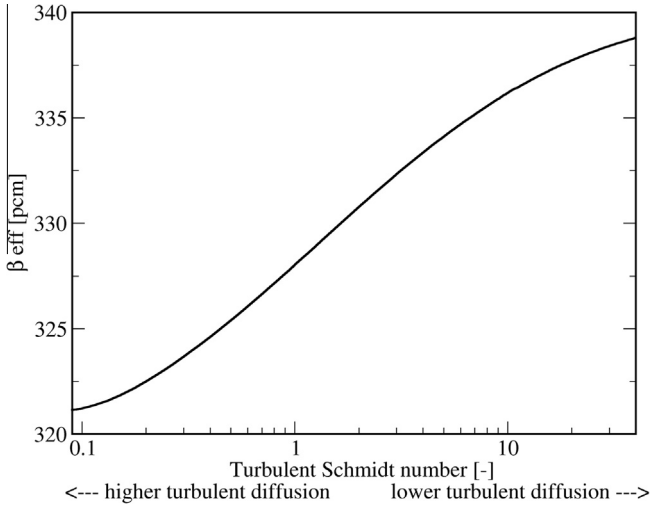

Fig. 9. Effective delayed neutron fraction as function of the turbulent Schmidt number Sc_T (U235-started, k-epsilon case study; nominal flow rate; OpenFOAM).

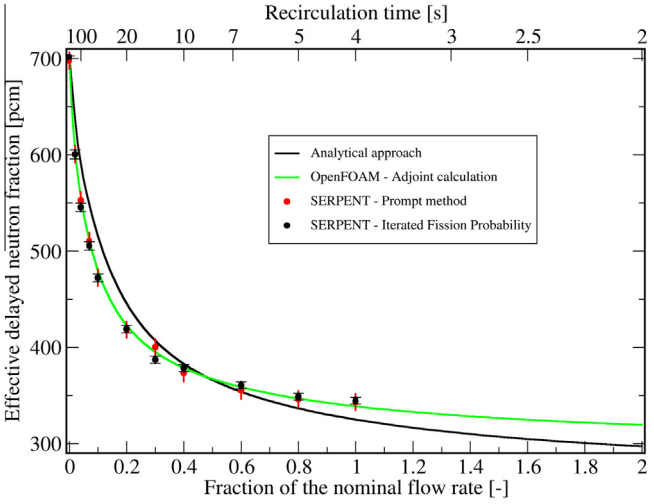

Fig. 10. Effective delayed neutron fraction in the MSFR as function of the flow rate: comparison between analytical approach, SERPENT and OpenFOAM (U235-started, k-epsilon case study; no turbulent diffusion).

comparison between different approaches. Nonetheless, while studying reactor neutronic characteristics, the expression of β_{eff} as function of the fuel flow rate might lead to more useful results. These data can be used to estimate the reactivity insertion/extraction as consequence of operational or accidental change in the behaviour of fuel pumps.

In Fig. 10, the effective delayed neutron fraction is plotted against the flow rate and circulation time. Around nominal flow rate conditions (about 4 s of recirculation time), the reactivity loss due to fuel circulation is close to saturation and only little reactivity is inserted/removed by small variation of the flow rate. At higher recirculation time, little modifications in the operating conditions cause high reactivity insertion/removal. OpenFOAM results show a good agreement with Monte Carlo estimations. SERPENT-2 calculations adopting the IFP method are always statistically compatible with the more expensive results of the "prompt" method. Starting from nominal flow rate, blockage of the pumps might lead to the slow insertion of slightly more that 350 pcm of reactivity if stagnation conditions are reached at the end of the transient. Predictions of the analytical approach can be considered a good approximation over the range between static fuel and nominal conditions, also because the errors due to fuel recirculation shown before for fast and slow groups partially compensate each other.

The adoption of the IFP method allows a computationally cheap estimation of the single effective delayed neutron fractions $\beta_{eff,i}$. In Figs. 11 and 12, the $\beta^c_{eff}/\beta^s_{eff}$ correction factor is shown for the different delayed neutron groups of the JEFF-3.1 library as function of the MSFR flow rate. At the top of the plots the corresponding fuel loop circulation time (T) is shown. For better clarity, the groups are divided in slow and fast. In Fig. 11, only the interval 0–10% of the flow rate is shown. Slower groups reach their saturation values already at very low flow rate. At nominal conditions, the correction factor is significantly greater than 0.5 only for groups 7 and 8.

In Fig. 13, delayed neutron fraction values are shown for different fuel compositions. The reduction in the values from β_{zero} to β^s_{eff} is due to differences in the energy spectra of prompt and delayed neutrons and is well captured by the Meulekamp and van der Marck (2006) method already available in SERPENT. In order to catch the effect of fuel motion, appropriate techniques are required (e.g., prompt or IFP methods). Energy effects are smaller and are dependent on the isotopic composition of the fissile material. Spatial effects are dominant and have a minor dependence on the fuel

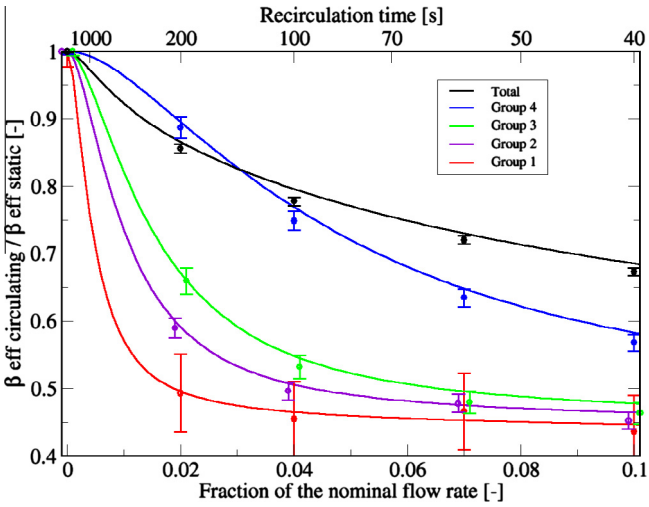

Fig. 11. $\beta^{c}_{i,eff}/\beta^{s}_{i,eff}$ correction factors. Solid line: OpenFOAM; dots: SERPENT (U235-started, k-epsilon case study; no turbulent diffusion).

composition. In particular, $\beta^{c}_{i,eff}/\beta^{s}_{i,eff}$ correction factors calculated for the different delayed neutron groups can be considered of a certain generality, because the decay constants λ_i of the JEFF-3.1 library are not dependent on the fuel composition. Moreover, spatial and energy effects may be separated as first approximation, in the case of the MSFR.

In Fig. 14, the spatial dependency of the delayed and prompt neutron source is shown as calculated with OpenFOAM for the 3D optimized MSFR core shape at nominal flow rate conditions. The delayed neutron source is calculated as sum over the eight delayed neutron groups. The upward shift of the fast decaying precursors is evident. The absence of in-core recirculation paths avoids precursors retention near reactor radial wall, as found in results related to the cylindrical axial-symmetric case study.

The optimized geometry and the simple cylindrical geometry have the same nominal in-core-to-total volume ratio (∼50%). The definition of in-core is problematic in this kind of reactors. In the out-of-core part of the fuel circuit the neutron flux is several order of magnitude lower than the average value of the core. Nonetheless, the transition between the two zones is not sharp and defined as in solid-fuelled reactors or even graphite-moderated molten salt reactors. For simplicity, the core volume is often considered as the whole region between piping inlets and outlets, having a volume of

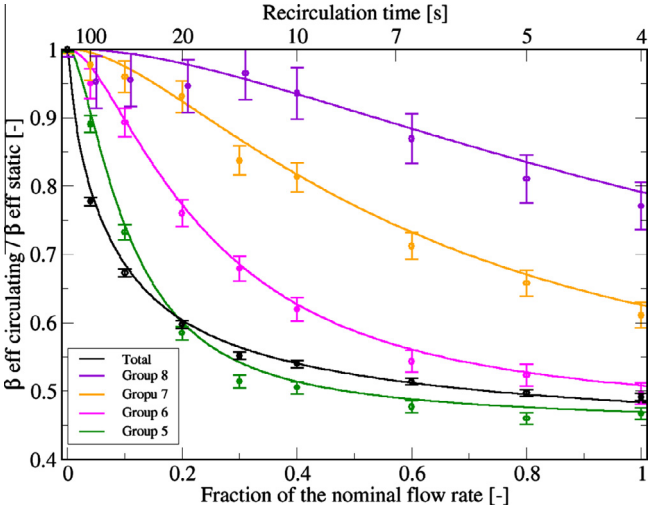

Fig. 12. $\beta^{c}_{i,eff}/\beta^{s}_{i,eff}$ correction factors. Solid line: OpenFOAM; dots: SERPENT (U235-started, k-epsilon case study; no turbulent diffusion).

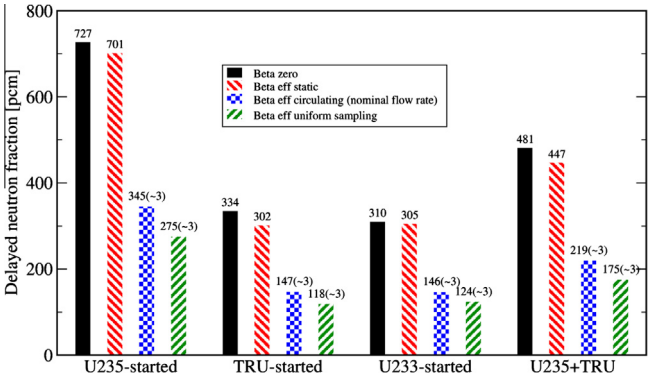

Fig. 13. Delayed neutron fractions in the MSFR for different fuel compositions.

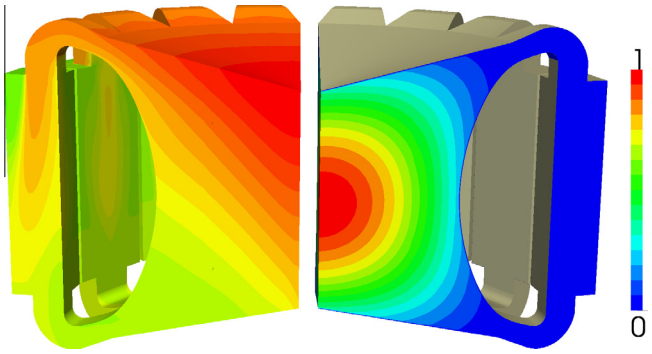

Fig. 14. Spatial distribution of the delayed (left) and prompt (right) neutron sources at nominal flow rate (arbitrary unit; OpenFOAM; optimized geometry, 3D case study; nominal flow rate).

approximately 9 m^3 for both the reference cylindrical and the optimized MSFR geometry. On the other hand, in Fig. 14, high leakage zones near core inlets and outlets with low neutron flux can be appreciated. If we consider as in-core volume the region having a neutron importance equal or greater than the 5% of the peak value, significant differences between the two geometries arise. The effective core volume calculated in this way results to be about 9.18 m^3 for the cylindrical axial-symmetric geometry and 7.92 m^3 for the optimized geometry, and the effective in-core-to-total volume ratio are 51% and 44%, respectively.

In Table 5, the results of the OpenFOAM simulations in the optimized geometry for different flow rates are presented. As discussed in Section 3, the analytical approach has been derived under the hypotheses of cylindrical core and uniform in-core axial velocity and does not allow for turbulent diffusion. Nonetheless, analytical results show a relative error with respect to OpenFOAM lower than 10% in the wide range from 0.3 to 1.5 of the nominal flow rate. If the effective in-core-to-total volume ratio calculated above (44%) is adopted, errors of about 3% are achieved.

5. Conclusions

The effective delayed neutron fraction is an important reactor kinetics parameter, whose calculation is particularly difficult in circulating-fuel reactors. A correct importance-weighting of the delayed neutron source has proved necessary to achieve accurate results. Approximate techniques have been often adopted in the literature, which proved inaccurate in the considered test case of the Molten Salt Fast Reactor. In this work, three different approaches have been presented and adopted to study the MSFR with different geometry and flow rate conditions. The extension of the

Table 5
Effective delayed neutron fraction in the optimized geometry for different flow rates. Comparison between OpenFOAM and the analytical approach (U235-started, optimized geometry, 3D case study).

Frac. of the flow rate (–)	Recirc. time (s)	OpenFOAM β_{eff} (pcm)	Analytical – $\gamma = 0.5$		Analytical – $\gamma = 0.44$	
			β_{eff} (pcm)	Rel. diff. (%)	β_{eff} (pcm)	Rel. diff. (%)
0.3	13.3	370.6	407.2	(+9.88)	378.2	(+2.05)
0.5	8	335.1	366.3	(+9.31)	335.4	(+0.09)
0.7	5.7	316.4	344.4	(+8.85)	312.7	(−1.17)
0.85	4.7	307.0	333.4	(+8.56)	301.3	(−1.86)
1	4	299.8	325.1	(+8.44)	292.7	(−2.37)
1.15	3.5	294.3	318.4	(+8.19)	285.9	(−2.85)
1.3	3.1	289.8	313.1	(+8.04)	280.4	(−3.24)
1.5	2.7	285.0	307.3	(+7.82)	274.5	(−3.68)

continuous energy Monte Carlo code SERPENT-2 involves the tracking of precursors according to an input velocity field. The effective delayed neutron fraction in circulating-fuel conditions is then calculated adopting the Iterated Fission Probability method. A deterministic approach is presented as well, which is based on the OpenFOAM multi-physics finite-volume tool-kit, and involves the solution of the multi-group diffusion forward and adjoint eigenvalue problems. The new solver allows for the convective and turbulent diffusive terms in the delayed neutron precursors balance. An analytical formula for the circulating-to-static effective delayed neutron fraction correction factor is also presented. The formula is derived under simple hypotheses for cylindrical geometries. It takes into account the effect of the fuel motion on the effective delayed neutron fraction due to the non-uniform spatial neutron importance.

Results of the comparison show a good agreement between the Monte Carlo and the deterministic approaches in the three analysed case studies. The analytical formula shows close agreement with OpenFOAM for the case study with simple geometrical and velocity field conditions. Moreover, it offers a good approximation even in conditions far from the hypotheses under which it was derived, and gives better results than the commonly adopted analytical approaches (without importance weighting) in all the analysed cases.

The effect of in-core flow recirculation has been studied, revealing that it is responsible of a relevant increase of the effective delayed neutron fraction, due to in-core retention of slow-decaying precursors. β_{eff} revealed to be dependent on the particular geometry and flow conditions. At nominal flow rate, differences of about 10% have been found for the analysed case studies with the same nominal in-core-to-total volume ratio of 50%. Results highlighted the importance of a proper solution of the fluid flow inside the core for an accurate calculation of the effective delayed neutron fraction.

The present OpenFOAM implementation of the eigenvalue problem involves the same spatial discretization for both the neutron diffusion and the precursor convection, which prevents the adoption of optimised meshes. Suitable conservative mapping techniques are available (e.g., Menon and Schmidt, 2011) and their adoption in future developments of the present work would allow a more efficient solution on separated meshes.

Higher-order methods for integration of stochastic differential equations (e.g., see Higham, 2001), possibly along with variable time-stepping techniques (e.g., see Gaines and Lyons, 1997), might be adopted in the presented Monte Carlo approach to accurately treat precursor turbulent diffusion.

An *Octave/Matlab* script which numerically integrates Eq. (5) to calculate the correction factor for circulating-fuel reactors is available upon request.

Acknowledgements

The authors would like to thank Jaakko Leppänen (VTT – Finland) for his precious collaboration about the generation of adjoint-weighted kinetics parameters with SERPENT and Carlo Fiorina (PSI – Switzerland) for fruitful discussions.

This work was financially supported by Politecnico di Milano via the PhD grant of Manuele Aufiero entitled "International Mobility 2012/2013", in the frame of the Doctoral Program in "Energy and Nuclear Science and Technology – 26 cycle".

This work has also been supported by CINECA supercomputing center under ISCRA Project MPMCF – *Multi-Physics Modelling of Circulating-Fuel Nuclear Reactors*, by Regione Lombardia and CILEA supercomputing center under LISA Project CFMC – *Simulazioni Monte Carlo per reattori a sali fusi*, and by an Amazon Web Services (AWS) in Education grant award.

References

Bell, G.I., Glasstone, S., 1979. Nuclear reactor theory. RE Krieger Publishing Company.

Brovchenko, M., Heuer, D., Merle-Lucotte, E., Allibert, M., Capellan, N., Ghetta, V., Laureau, A., 2012. Preliminary safety calculations to improve the design of Molten Salt Fast Reactor. In Proceedings of PHYSOR 2012. Knoxville, TN, USA, April 15–20, 2012.

Cammi, A., Di Marcello, V., Guerrieri, C., Luzzi, L., 2011. Transfer function modeling of zero-power dynamics of circulating fuel reactors. Journal of Engineering for Gas Turbines and Power 133 (5), 052916-1–052916-8.

Carta, M., Dulla, S., Peluso, V., Ravetto, P., Bianchini, G., 2011. Calculation of the effective delayed neutron fraction by deterministic and Monte Carlo methods. Science and Technology of Nuclear Installations 2011, 8.

Clifford, I., Ivanov, K., 2010. PBMR 400 MW benchmark calculations using the simplified P_3 approach. In: Proceedings of HTR2010. Prague, Czech Republic, October 18–20, 2010.

Clifford, I., Jasak, H., 2009. The application of a multi-physics toolkit to spatial reactor dynamics. In: 2009 International Conference on Mathematics, Computational Methods & Reactor Physics (M&C 2009). Saratoga Springs, NY, USA, May 3–7, 2009.

Doligez, X., 2010. Influence du retraitement physico-chimique du sel combustible sur le comportement du MSFR et sur le dimensionnement de son unité de retraitement, Ph.D. thesis, Institut National Polytechnique de Grenoble-INPG.

Dormand, J.R., Prince, P.J., 1980. A family of embedded Runge–Kutta formulae. Journal of Computational and Applied Mathematics 6 (1), 19–26.

EVOL, 2010–2013. Evaluation and Viability Of Liquid Fuel Fast Reactor System. <http://www.evol-project.org/>.

Fiorina, C., Aufiero, M., Cammi, A., Franceschini, F., Krepel, J., Luzzi, L., Mikityuk, K., Ricotti, M.E., 2013. Investigation of the MSFR core physics and fuel cycle characteristics. Progress in Nuclear Energy 68, 153–168.

Gaines, J.G., Lyons, T.J., 1997. Variable step size control in the numerical solution of stochastic differential equations. SIAM Journal on Applied Mathematics 57 (5), 1455–1484.

GIF, 2010. Generation IV International Forum. Annual Report. <http://www.gen-4.org/PDFs/GIF-2010-Annual-Report.pdf>.

Guerrieri, C., Aufiero, M., Cammi, A., Fiorina, C., Luzzi, L., 2012. A preliminary study of the MSFR dynamics. In: Proceedings of ICONE20. Anaheim, CA, USA, July 30–August 3, 2012.

Guerrieri, C., Cammi, A., Luzzi, L., 2013. An approach to the MSR dynamics and stability analysis. Progress in Nuclear Energy 67 (0), 56–73 (ISSN 0149-1970).

Higham, D.J., 2001. An algorithmic introduction to numerical simulation of stochastic differential equations. SIAM Review 43 (3), 525–546.

Kiedrowski, B.C., 2012. Impact of delayed neutron precursor mobility infissile solution systems. In: Proceedings of PHYSOR 2012. Knoxville, TN, USA, April 15–20, 2012.

Kiedrowski, B.C., Brown, F.B., Wilson, P.P., 2011. Adjoint-weighted tallies for k-eigenvalue calculations with continuous-energy Monte Carlo. Nuclear Science and Engineering 168 (3), 226–241.

Koning, A., Forrest, R., Kellett, M., Mills, R., Henriksson, H., Rugama, Y., 2006. The JEFF-3.1 Nuclear Data Library, Technical Report, JEFF Report 21. NEA – OECD.

Kópházi, J., Szieberth, M., Fehér, S., Czifrus, S., de Leege, P.F., 2004. Monte Carlo calculation of the effects of delayed neutron precursor transport in molten salt reactors. In: Proceedings of PHYSOR 2004. Chicago, IL, USA, April 25–29, 2004.

Kópházi, J., Lathouwers, D., Kloosterman, J., 2009. Development of a three-dimensional time-dependent calculation scheme for molten salt reactors and validation of the measurement data of the molten salt reactor experiment. Nuclear Science and Engineering 163 (2), 118–131.

Lapenta, G., Mattioda, F., Ravetto, P., 2001. Point kinetic model for fluid fuel systems. Annals of Nuclear Energy 28 (17), 1759–1772.

Lecarpentier, D., 2001. Le concept AMSTER, aspects physiques et sûreté, Ph.D. thesis, Conservatoire National des Arts et Métiers.

Leppänen, J., Aufiero, M., Fridman, E., Rachamin, R., van der Marck, S. 2013. Calculation of effective point kinetics parameters in the Serpent 2 Monte Carlo code. Annals of Nuclear Energy (this issue).

Mattioda, F., Ravetto, P., Ritter, G., 2000. Effective delayed neutron fraction for fluid-fuel systems. Annals of Nuclear Energy 27 (16), 1523–1532.

Menon, S., Schmidt, D.P., 2011. Conservative interpolation on unstructured polyhedral meshes: an extension of the supermesh approach to cell-centered finite-volume variables. Computer Methods in Applied Mechanics and Engineering 200 (41), 2797–2804.

Merle-Lucotte, E., Heuer, D., Allibert, M., Doligez, X., Ghetta, V., 2009. Optimizing the burning efficiency and the deployment capacities of the Molten Salt Fast Reactor. In: Proceedings of GLOBAL 2009. Paris, France, September 6–11, 2009.

Merle-Lucotte, E., Heuer, D., Allibert, M., Brovchenko, M., Capellan, N., Ghetta, V., 2011. Launching the thorium fuel cycle with the Molten Salt Fast Reactor. In: Proceedings of ICAPP 2011. Nice, France, May 2–6, 2011.

Merle-Lucotte, E., Heuer, D., Allibert, M., Brovchenko, M., Ghetta, V., Rubiolo, P., Laureau, A., et al. 2013. Recommandations for a demonstrator of Molten Salt Fast Reactor. In: International Conference on Fast Reactors and Related Fuel Cycles: Safe Technologies and Sustainable Scenarios (FR13). Paris, France, March 4–7 2013.

Meulekamp, R.K., van der Marck, S.C., 2006. Calculating the effective delayed neutron fraction with Monte Carlo. Nuclear Science and Engineering 152 (2), 142–148.

Nagaya, Y., Chiba, G., Mori, T., Irwanto, D., Nakajima, K., 2010. Comparison of Monte Carlo calculation methods for effective delayed neutron fraction. Annals of Nuclear Energy 37 (10), 1308–1315. http://dx.doi.org/10.1016/j.anucene.2010.05.017 (ISSN 0306-4549).

Nauchi, Y., Kameyama, T., 2010. Development of calculation technique for Iterated Fission Probability and reactor kinetic parameters using continuous-energy Monte Carlo method. Journal of Nuclear Science and Technology 47 (11), 977–990.

Rollet, A.-L., Sarou-Kanian, V., Bessada, C., 2010. Self-diffusion coefficient measurements at high temperature by PFG NMR. Comptes Rendus Chimie 13 (4), 399–404.

Rudstam, G., Finck, Ph., Filip, A., D'Angelo, A., McKnight, R.D., 2002. Delayed Neutron Data for the Major Actinides. NEA/WPEC-6 Report.

Sakurai, T., Okajima, S., Andoh, M., Osugi, T., 1999. Experimental cores for benchmark experiments of effective delayed neutron fraction β_{eff} at FCA. Progress in Nuclear Energy 35 (2), 131–156.

Salanne, M., Simon, C., Groult, H., Lantelme, F., Goto, T., Barhoun, A., 2009. Transport in molten LiF–NaF–ZrF4 mixtures: a combined computational and experimental approach. Journal of Fluorine Chemistry 130 (1), 61–66.

SERPENT, 2011. PSG2/Serpent Monte Carlo Reactor Physics Burnup Calculation Code. <http://montecarlo.vtt.fi>.

Tominaga, Y., Stathopoulos, T., 2007. Turbulent Schmidt numbers for CFD analysis with various types of flowfield. Atmospheric Environment 41 (37), 8091–8099.

Weller, H.G., Tabor, G., Jasak, H., Fureby, C., 1998. A tensorial approach to computational continuum mechanics using object-oriented techniques. Computers in Physics 12, 620–631.